ELSEVIER

Catalysis Today 56 (2000) 103–111

CATALYSIS TODAY

www.elsevier.com/locate/cattod

A carbon membrane reactor

N. Itoh *, K. Haraya

National Institute of Materials and Chemical Research, Tsukuba, 305-8565 Japan

Abstract

A carbon membrane reactor as one of the applications of carbon membranes was newly developed and examined using dehydrogenation of cyclohexane as a test reaction. Permeation of hydrogen, argon, cyclohexane and benzene through carbon membranes showed the so-called molecular-sieving like diffusion behavior. The performance of the carbon membrane reactor for the dehydrogenation was found to exceed that of a normal reactor, i.e., equilibrium conversion. ©2000 Elsevier Science B.V. All rights reserved.

Keywords: Carbon membrane; Hollow fiber; Membrane reactor; Dehydrogenation; Equilibrium shift

1. Introduction

During the last 5 years, increasing concerns have been focused on carbon membranes, which can be prepared basically by carbonizing organic polymers as starting materials at high-temperatures, since it is expected that carbonized materials can be stable at high-temperatures and resist chemical attack. So far, four types of carbon membranes, i.e., sheet [1–4], capillary [5], hollow fiber [6–8] and composite [9–14], have been prepared. From the standpoint of large-scale applications, capillaries, hollow fibers and tubular composites will be preferable because of their high packing density (membrane area per unit volume of vessel) whereas sheets (disks) are confined to treatment of fine chemicals, etc., and use in laboratory. Of the three types, hollow fibers would be the best in terms of high area/volume ratio and easier module assembly. Additional advantage is that the carbonization of original polymer fibers with several hundred micrometers in diameter can be carried out in a continuous process [8]. Carbon hollow fiber membranes, having an asymmetric structure, showed a large permeability and a high selectivity for inorganic gases and light hydrocarbons [7,8]. Its application, therefore, is expected to spread over not only high-temperature separations but also membrane reactors.

Membrane reactors, in which a chemical equilibrium shift can be realized via selective product removal, have a possibility of playing an important role in establishing an energy-efficient process in the future petrochemical and chemical industries. Especially, palladium membrane reactors [15–22] have demonstrated their great performances for dehydrogenations, steam reforming reactions, etc., where only hydrogen is selectively separated from the reacting mixture, thereby realizing extremely high conversions over the equilibrium ones. However, it is often pointed out that palladium membranes have some problems in terms of cost and permeability when an industrial application of palladium membrane reactors is discussed. Such a condition will emphasize that other membrane materials alternative to palladium should be explored and developed. From this point of

* Corresponding author. Fax: +81-298-56-8587.
E-mail address: nitoh@nimc.go.jp (N. Itoh).

PII: S0920-5861(99)00267-9

view, one can expect that carbon membranes, gaining a great interest recently, become one of the candidates for the membrane material with high hydrogen permselectivity due to a molecular-sieving effect.

In this study, therefore, an application of carbon fiber membranes to a membrane reactor for dehydrogenation is experimentally discussed.

2. Experimental

2.1. Preparation of carbon fibers

As a starting material for the carbon fiber, asymmetric polyimide hollow fibers, which were supplied by UBE Industry, Japan, were employed. The fibers of 400 μm in diameter were carbonized according to the following treatment:

1. The polyimide fibers were treated in an air oven at 400°C for 30 min so as to maintain their asymmetric structure even when being exposed to higher temperatures. If this treatment is omitted, a softening will take place during the next step and then the asymmetric structure will be significantly damaged [8].
2. The pretreated fibers were pyrolyzed in a vacuum oven at 750°C for 60 min.

In Fig. 1, cross-sectional views of the original and carbonized fibers, observed with a field emission scanning microscope (FE-SEM), are shown. It is obvious that a sponge-like structure was mostly maintained even after carbonization although some shrinkage could be recognized.

2.2. Apparatus and experimental method

Fig. 2 is the schematic drawing of the carbon membrane reactor developed in this study. Twenty carbonized hollow fibers (0.295 μm in diameter, 128 mm long) were bundled, plugged on one side with a high-temperature adhesive, and housed inside a 10 mm (o.d.) porous sintered metal tube to protect from breaking, which was located at the center of the tubular reactor. Catalyst pellets (0.5 wt.% Pt/Al_2O_3) were packed in the concentric annular space between the 30 mm (i.d.) shell tube and the sintered tube.

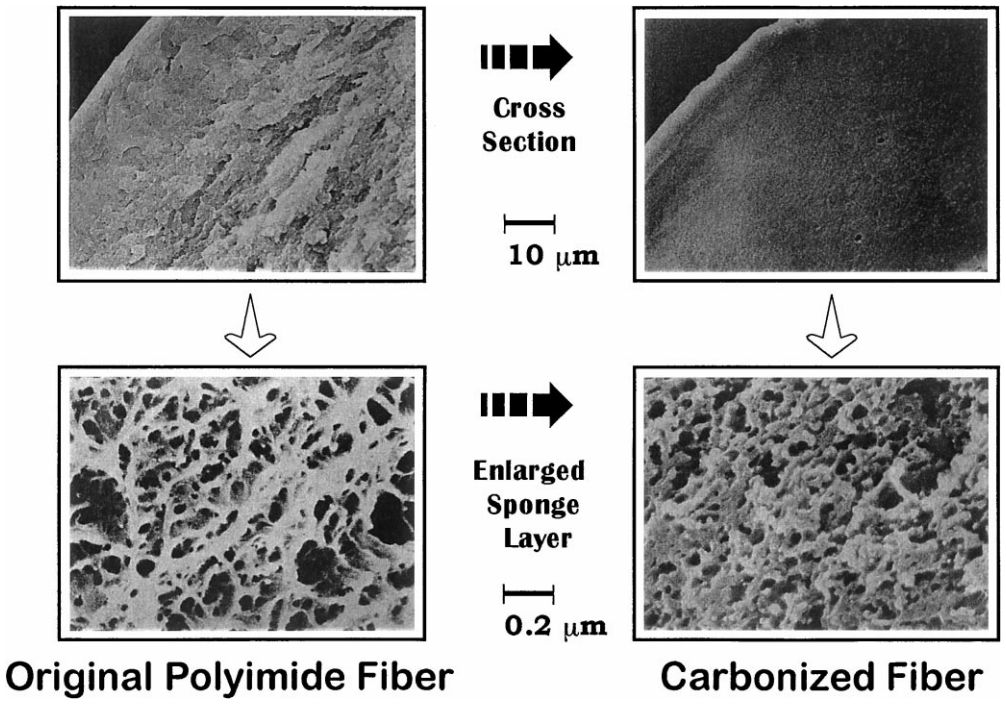

Fig. 1. Cross-sectional view (FE-SEM) of the fiber before and after carbonization.

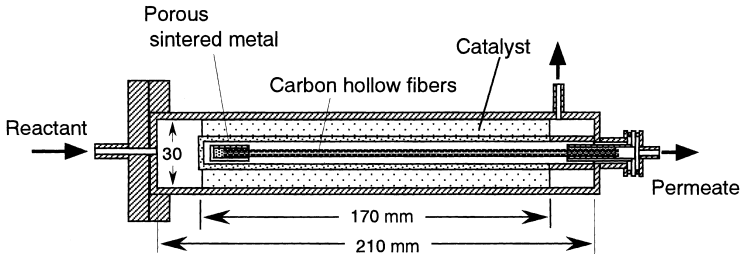

Fig. 2. Schematic of a carbon membrane reactor developed.

The carbon membrane reactor was placed inside an air oven type of thermostat as can be seen in Fig. 3. Argon gas as a carrier was supplied at a constant flowrate through a mass flow controller. The pressure inside the reactor, if necessary, was kept higher than atmospheric pressure with a back-pressure regulator.

Gas permeabilities of pure gases (H_2, Ar) were examined in the range 50–195°C. The flowrate of gas permeated from the shell side, which was held at a pressure higher than atmospheric pressure on the permeate side (pressurized mode), was measured with a soap-film flowmeter. Permeation rates of benzene and cyclohexane at 195°C were also measured using their mixtures with H_2 or Ar as feed. Measurements by the pressurized mode were first done using only argon (hydrogen), and then using a mixture with benzene, which was pumped into a vaporizer at a fixed rate. The test gases were sent to the shell side of the carbon membrane reactor with argon (hydrogen). After finishing the vapor permeation, argon (hydrogen) gas permeation was examined again.

Dehydrogenation of cyclohexane to benzene was taken as a test reaction and carried out at 195°C and atmospheric pressure. The liquid reactant was sent to a vaporizer with a syringe pump, and the evolved vapor entered the reactor together with argon as diluent. The effluent gas from the reactor was analyzed with a gaschromatograph. To obtain a driving force for separation in the case of operating the membrane reactor, the permeate side was kept at a reduced pressure with a vacuum type of pressure controller (evacuation mode). For comparison, the performance of a normal reactor, where the permeate side was closed and never evacuated, was examined (normal reactor mode).

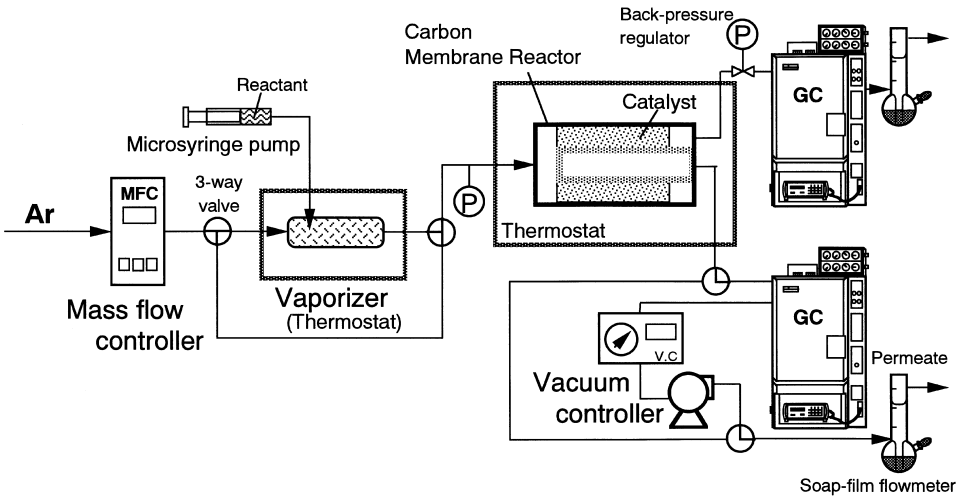

Fig. 3. Flow diagram of the experimental set-up.

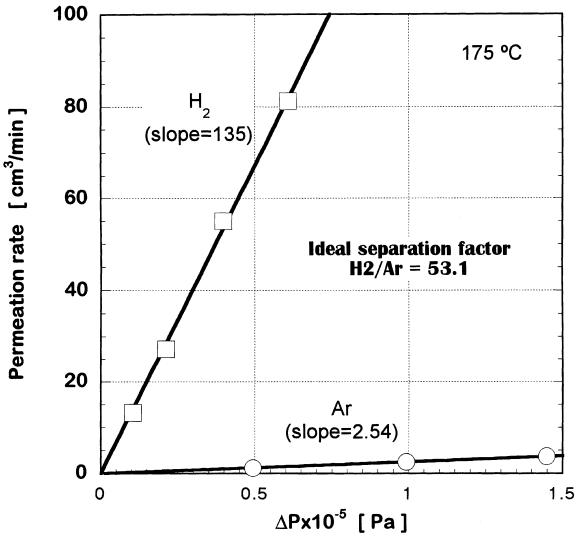

Fig. 4. Plots of permeation rate against transmembrane pressure.

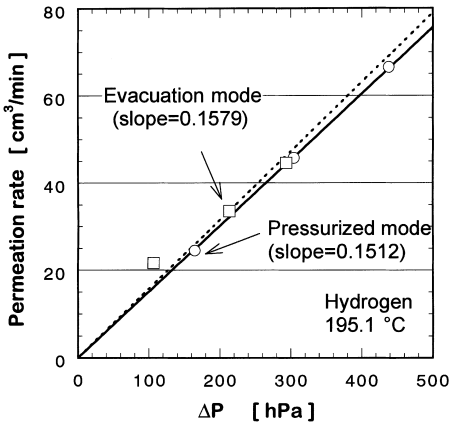

Fig. 5. Hydrogen permeation rate measured by two different modes.

3. Results and discussion

3.1. Permeation of single gas (H_2, Ar)

Fig. 4 shows the permeation rates of hydrogen and argon with varying transmembrane pressure at 175°C while the permeation side is kept at atmospheric pressure (pressurized mode). The ideal separation factor of 53.1 for H_2/Ar is obtained from comparing the slopes. Another way of measuring permeation rate is to keep the permeation side lower than atmospheric side by evacuating with a vacuum pump, where the permeation rate is measured with a soap-film flowmeter connecting to the exhaust of the vacuum pump. A comparison of hydrogen permeation rates between the pressurized and evacuation modes is made in Fig. 5. It can be said that both the results are in a good agreement, so that either of them can be good enough as the method of measurement.

The temperature dependency of the permeation rates is shown in Fig. 6. The permeation rate is obvious to increase exponentially with an increase of temperature, where the apparent activation energy for the argon permeation is larger than that for hydrogen. This means that the carbon membrane has micropores with an average diameter close to those of the gas molecules and therefore the permeation through it is based on the molecular-sieving like diffusion mechanism. The ideal separation factor, a ratio of permeation rate of H_2 to that of Ar, decreases with increasing temperature.

3.2. Permeation of benzene and cyclohexane

Single gas permeation tests of condensable gases like benzene and cyclohexane are difficult because the

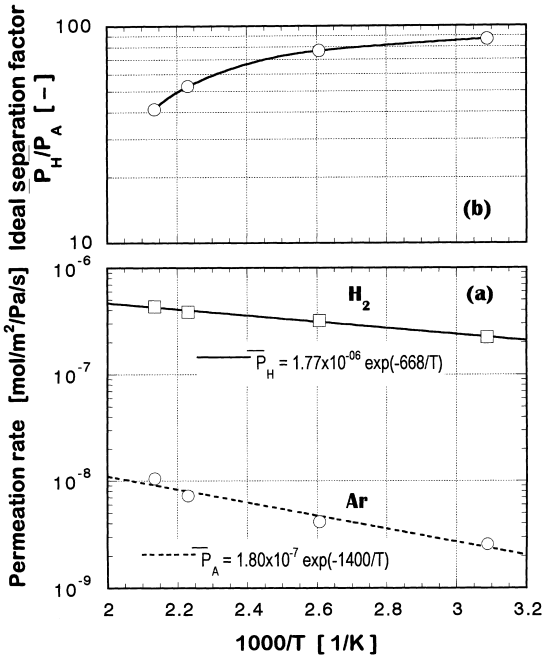

Fig. 6. Temperature dependence of (a) permeation rates of H_2 and Ar, and (b) ideal separation factor.

Table 1
Experimental conditions for measuring gas permeation rates in the binary mixture system

	C_6H_6–Ar system	C_6H_{12}–H_2 system
ΔP[a] (10^5 Pa)	0.556	0.226
Temperature (°C)	195.3	195.3
Flowrate of inorganic gas ($cm^3\,min^{-1}$) (STP)	45.8	39.1
Feed rate of organics ($mg\,min^{-1}$)	2.13	1.94

[a] Permeate side: atmospheric pressure.

condensation is apt to occur anywhere in the tubing, in which the temperature is close to or lower than the boiling points. This means that an accurate measurement of the flowrate of permeates is troublesome. Therefore, in this study, the permeation rate was determined by the following procedure.

Benzene–argon system: First, the single gas permeation of argon was carried out by the pressurized mode to obtain the permeation rate. Then, benzene was added in the argon flow with a microsyringe pump constantly. The effluent gas on the permeate side was analyzed by gaschromatography to obtain the concentration of benzene in the permeate stream, followed by measuring the flowrate. The benzene permeation rate can thus be calculated by multiplying the flowrate by the concentration of benzene. The detailed experimental conditions are shown in Table 1. After finishing the binary-mode measurement, the second single gas permeation test for argon was made to compare with the first result.

Cyclohexane–H_2 system: Cyclohexane cannot be used since being easily dehydrogenated to benzene. Then a H_2–benzene binary mixture, which could be completely converted to cyclohexane as soon as entering inside the reactor, was employed as feed. The method to determine the permeation rates under the conditions as shown in Table 1 is similar to that of the benzene–argon system.

The permeation rates measured for H_2 and Ar are shown in Fig. 7. It is found that the permeation rates of single gases, H_2 and Ar, are unchanged before and after the binary mixture permeation while those measured in the presence of the organic vapor are significantly decreased. But this decrease was only observed initially, and therefrom a steady permeation rate could be obtained. Table 2 gives the permeation rate of each gas species in the binary-mode. It can be seen that the permeation rates of H_2 and Ar decrease by

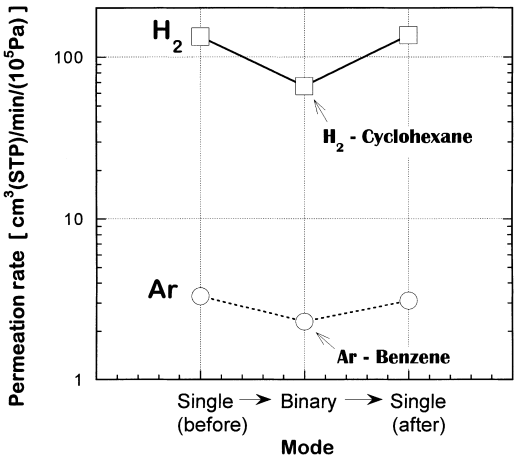

Fig. 7. Comparison of permeation rates of single gases with those when benzene or cyclohexane vapor was fed together (195.3°C).

about 50 and 25%, respectively, compared with those in the single gas mode. Cyclohexane permeates 1/25 times as slowly as argon, and 1/730 times as hydrogen. Benzene permeation was very little and difficult to be identified because a peak recorded with the TCD detector of the gas chromatograph was too small.

An explanation possible for the above result would be as follows. It is considered that there should exist a distribution in the pore diameter of the carbon

Table 2
Permeation rates Q_i ($cm^3\,cm^{-2}\,min^{-1}$ (10^{-5} Pa)) (STP) measured at 195.3°C

Gas i	Single gas permeation		Binary gas permeation	
	Q_i	Q_{H_2}/Q_i	Q_i	Q_{H_2}/Q_i
H_2	5.41	1	2.69	1
Ar	0.126	42.9	0.0935	28.8
C_6H_{12}	–	–	0.0369	729
C_6H_6	–	–	Trace[a]	–

[a] As a result of GC analysis with a TCD detector.

membrane used. If micropores larger than benzene and cyclohexane molecules are plugged by either adsorption or condensation of the organic molecules, they can no longer be used as permeation channels for the inorganic gases, as well as the organic molecule itself. Since the kinetic diameters are 0.6 nm for benzene, 0.585 nm for cyclohexane, 3.4 nm for Ar and 2.89 nm for H_2, respectively, the inorganic gases smaller than the organic gases can permeate through the smaller micropores, which are never filled by the organic molecules. This would be why the permeation rates of H_2 and Ar dropped during the binary-mode measurement.

3.3. Dehydrogenation using carbon membrane reactor

3.3.1. Mathematical model

When plug flow, no mixing diffusion, isobaric and isothermal conditions are assumed, changes of flowrate for each component along the axial direction of the carbon membrane reactor can be described by simultaneous ordinary differential equations as summarized in Table 3. A set of the fundamental equations can be solved numerically by using the Runge–Kutta–Gill method if the kinetic parameters are known. In this study, the rate constant, k_r, and the adsorption constant, K_B, in the literature [23] were used.

Table 3
Ideal mathematical model governing the flowrate change of each component in the reaction, C = B + 3H, progressing along the carbon membrane reactor

Reaction side	
$dU_C/dL = -Da \cdot f_r - T_C(m_C - \beta n_C)$	(1)
$dU_B/dL = -Da \cdot f_r - T_B(m_B - \beta n_B)$	(2)
$dU_H/dL = 3Da \cdot f_r - T_H(m_H - \beta n_H)$	(3)
$dU_I/dL = -T_I(m_I - \beta n_I)$	(4)
Permeation side	
$dV_C/dL = -T_C(m_C - \beta n_C)$	(5)
$V_B = 1 - U_C - U_B - V_C$	(6)
$V_H = 3(1 - U_C - V_C) - U_H$	(7)
$V_I = \alpha - U_I$	(8)
Initial conditions	
at $L = 0$: $U_C = 1$, $U_I = \alpha$,	
$U_B = U_H = V_C = V_B = V_H = V_I = 0$	
$f_r = (K_p m_C/P_r^3 - m_B m_H^3)/(m_H^3 + K_B K_p m_C/P_r^2)$	(9)
$T_i = Q_i A P_r/u_C^0$	(10)
$Da = k_r P_r V_r/u_C^0$	(11)
$\alpha = u_I^0/u_C^0$, $\beta = P_s/P_r$	(12)

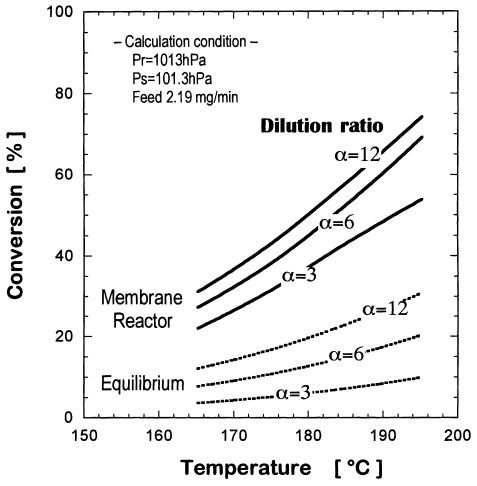

Fig. 8. Effect of dilution ratio on the conversion.

First, the performance of the carbon membrane reactor is predicted and compared with the equilibrium conversion in Fig. 8, where H_2 and Ar are assumed to permeate at their permeation rates in the single gas mode noted in Table 2and the permeation rates of benzene and cyclohexane are assumed to be negligibly small. The reason why higher conversions are obtained is, of course, because hydrogen as one of the products is selectively separated from the reacting mixture. However, it is noted that as the dilution ratio, α, increases, the increasing rate in the conversion attained by the carbon membrane reactor somewhat decreases. This is attributed to a higher permeation of argon. It is evident that argon added to cyclohexane should lead to an increase in conversion due to a dilution effect for a reaction system with an increase in the number of moles. Accordingly, the permeation of inert gas results in a reverse effect, i.e., depressing the conversion.

Next, the conversions calculated using the permeation rates measured in the binary-mode (Table 2) are compared with those in the single mode in Fig. 9. The latter is found to be always higher than the former. The difference becomes larger with decreasing pressure on the separation side. This is because the reducing pressure gives a raise in the permeation flux and therewith cyclohexane, an undesired permeate, also moves from the reaction to the separation side. Clearly, such cyclohexane permeation results in a loss in the conversion.

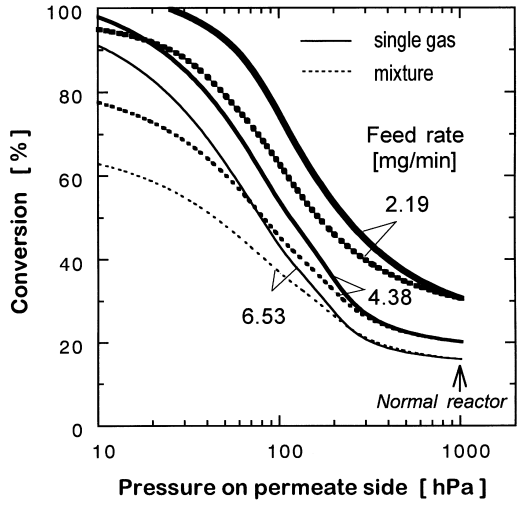

Fig. 9. Comparison of conversions predicted on the basis of single gas permeation with those of mixed gas permeation (195.2°C, 1014 h Pa, Ar 7.60 ml min^{-1}).

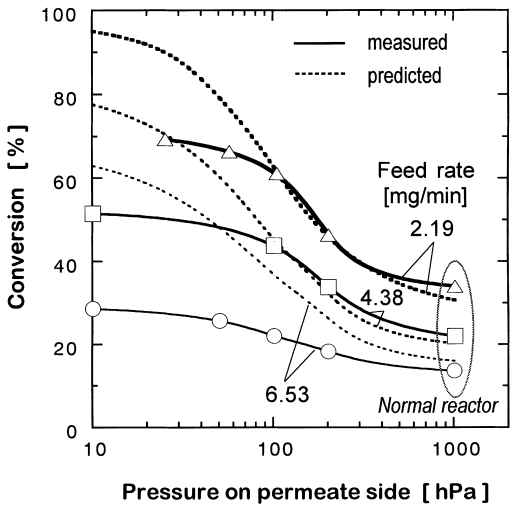

Fig. 11. Comparison of measured conversions with those predicted (195.2°C, 1014 h Pa, Ar 7.60 ml min^{-1}).

3.3.2. Experimental results and comparison with predictions

The effect of feed rate on the conversion is shown in Fig. 10. It is obvious that as the feed rate decreases, i.e., increasing residence time of the feed, the conversion increases. Moreover, as expected from the prediction above, higher conversions exceeding the equilibrium ones are attained. This is, of course, a chemical equilibrium shift due to a preferential permeation of hydrogen, one of the products in the cyclohexane dehydrogenation.

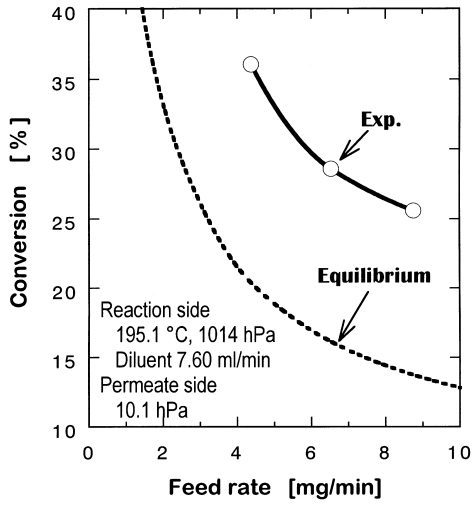

Fig. 10. Effect of feed rate on the reactor performance.

Fig. 11 shows a comparison between experimental data and the predictions with respect to the performance of the carbon membrane reactor with varying feed rate as well as permeation side pressure. The reason for an increase in conversion with decreasing feed rate is the same as the above discussion (Fig. 10). A rise in conversion with decreasing pressure on the permeate side is due to increasing amount of hydrogen separated selectively. In the normal reactor mode, the performance of which is represented by the plots near 1000 h Pa, it is found that the conversions attained are very close to the corresponding equilibrium conversions. Apparently the deviation between the data and the prediction lines becomes larger with increasing feed rate and with decreasing permeate side pressure. Still, a good coincidence between both can be found in the range over 100–1000 h Pa of the permeate side pressure when the feed rates are 2.19 and 4.38 mg min^{-1}. Such better prediction results, although within a limited range, suggest that the ideal flow assumption made to derive the analytical model in Table 3 is mostly valid.

On the other hand, it can be seen that the increasing rate of the conversion with decreasing permeate side pressure slows down in the range of 10–100 h Pa, and the deviation between both the lines becomes large.

Although making a clear explanation for this result is difficult at present, one of the major reasons conceivable is a decrease in the flux of hydrogen, i.e., caused by the so-called concentration polarization (distribution) with hydrogen in the radial direction [23–25], suggesting that the practical flow deviates from the ideal flow. To prove this, however, further study including development of a more precise mathematical model to analyze the combined reaction and separation occurring within the carbon membrane reactor should be necessary. Simultaneously, improving the reactor configuration will be important to minimize the influence of the concentration polarization. Furthermore, it should be inquired whether any change in the activity of the catalyst under such an unusual condition, i.e., a hydrogen concentration lower than that at the equilibrium composition, occurs because the catalyst is apt to lose its activity in a less hydrogen atmosphere.

4. Conclusions

A carbon membrane reactor promising as one of the applications of carbon membranes was newly developed, and its performances in the gas separation and the dehydrogenation of cyclohexane to benzene were examined.

Permeation rates of hydrogen, argon, cyclohexane and benzene through the carbon membrane, made of a bundle of 20 carbon fibers, were molecular-sieving like diffusion controlled. During the reaction experiments, cyclohexane and benzene, much less permeable components, were only detected as a trace using a gas chromatograph with a TCD detector.

The performance of the carbon membrane reactor for the dehydrogenation was fairly good compared with that of a normal reactor, i.e., equilibrium conversion. The mathematical model derived on the assumption of ideal flow could explain the experimental data within a limited range of the reaction condition. Beyond the range, however, the data deviated significantly from the predictions. As the major reasons, it was pointed out that a radial concentration polarization of hydrogen depressed the conversion, and any change in the activity of the catalyst occurred under a less hydrogen atmosphere.

5. Nomenclature

Da	Damköhler number, $k_r V_r P_r / u_C^0$ (−)
f_r	rate expression given by Eq. (9) in Table 3 (−)
k_r	rate constant of dehydrogenation (mol m^{-3} s^{-1} Pa^{-1})
K_B	adsorption equilibrium constant (Pa^{-1})
K_p	equilibrium constant for dehydrogenation (Pa^3)
l_e	entire reactor length (m)
L	dimensionless reactor length, l/l_e (−)
m_i	mole fraction of gas i on the reaction side, p_i/P_r (−)
n_i	mole fraction of gas i on the separation side, p_i/P_s (−)
p_i	partial pressure of gas i (Pa)
P_r	total pressure on the reaction side (Pa)
P_s	total pressure on the separation side (Pa)
Q_i	permeability of gas i (mol m^{-2} s^{-1} Pa^{-1})
T_i	dimensionless number given by Eq. (10) in Table 3 (−)
u_i	flowrate of gas i in the reaction-side stream (mol s^{-1})
u_C^0	flowrate of reactant at the reaction-side inlet (mol s^{-1})
U_i	dimensionless flowrate of gas i, u_i/u_C^0 (−)
v_i	flowrate of gas i in the separation-side stream (mol s^{-1})
V_r	reaction-side volume (m^3)
V_i	dimensionless flowrate of gas i, v_i/u_C^0 (−)
α	dilution ratio (−)
β	pressure ratio (−)

Subscripts

C	reactant, cyclohexane
B	dehydrogenated product, benzene
H	hydrogen
I	inert
i	gas i
r	reaction side
s	separation side

References

[1] H. Suda, K. Haraya, J. Phys. Chem. B 101 (1997) 3988.
[2] W. Shusen, Z. Meiyun, W. Zhizhong, J. Membr. Sci. 109 (1996) 267.

[3] H. Suda, K. Haraya, J. Chem. Soc., Chem. Commun. (1997) 93.
[4] H. Kita, M. Yoshino, K. Okamoto, Chem. Commun. 11 (1997) 1051.
[5] J. Petersen, M. Matsuda, K. Haraya, J. Membr. Sci. 131 (1997) 85.
[6] V.M. Linkov, R.D. Sanderson, E.P. Jacobs, J. Membr. Sci. 93 (1994) 93.
[7] V.C. Geiszler, W.J. Koros, Ind. Eng. Chem. Res. 35 (1996) 2999.
[8] Y. Kusuki, H. Shimazaki, N. Tanihara, S. Nakanishi, T. Yoshinaga, J. Membr. Sci. 134 (1997) 245.
[9] M.B. Rao, S. Sircar, J. Membr. Sci. 85 (1993) 253.
[10] Y.D. Chen, R.T. Yang, Ind. Eng. Chem. Res. 33 (1994) 3146.
[11] S. Morooka, J. Hayashi, H. Mizuta, Ind. Eng. Chem. Res. 35 (1996) 4176.
[12] M.B. Rao, S. Sircar, J. Membr. Sci. 110 (1996) 109.
[13] H. Kita, H. Maeda, K. Okamoto, Chem. Lett. 2 (1997) 179.
[14] J. Hayashi, M. Yamamoto, K. Kusakabe, S. Morooka, Ind. Eng. Chem. Res. 36 (1997) 2134.
[15] J. Shu, B.P.A. Grandjean, A. Van Neste, S. Kaliaguine, Can. J. Chem. Eng. 69 (1991) 1036.
[16] J. Shu, B.P.A. Grandjean, S. Kaliaguine, Appl. Catal. A 119 (1994) 305.
[17] A.M. Adris, C.J. Lim, J.R. Grace, Chem. Eng. Sci. 49 (1994) 5833.
[18] N. Itoh, Catal. Today 25 (1995) 351.
[19] E. Kikuchi, Sekiyu Gakkaishi 39 (1996) 301.
[20] E. Gobina, R. Hughes, Appl. Catal. A 137 (1996) 119.
[21] J.K. Ali, A. Baiker, Appl. Catal. A 155 (1997) 41.
[22] G. Barbieri, V. Violante, F.P.Di. Mario, A. Cirscuoli, E. Drioli, Ind. Eng. Chem. Res. 36 (1997) 3369.
[23] N. Itoh, T.H. Wu, J. Membr. Sci. 124 (1997) 213.
[24] N. Itoh, W.C. Xu, K. Harya, Ind. Eng. Chem. Res. 33 (1994) 197.
[25] T.H. Wu, N. Itoh, Chem. Eng. (China) 25 (1997) 22.